Design of Conical DRH Antennas for K and Ka Frequency Bands

Aliakbar Dastranj,[1] Habibollah Abiri,[1] Alireza Mallahzadeh[2]

[1] Department of Communication and Electronics Engineering, School of Electrical and Computer Engineering, Shiraz University, Shiraz, Iran
[2] Department of Electrical Engineering, Faculty of Engineering, Shahed University, Tehran, Iran

Received 14 February 2011; accepted 25 April 2011

ABSTRACT: Two conical double-ridged horn (DRH) antennas for K and Ka frequency bands are presented. Detailed simulation and experimental investigations are conducted to understand their behaviors and optimize for broadband operation. The designed antennas were fabricated with 0.01 mm accuracy and satisfactory agreement of computer simulations and experimental results was obtained. The designed conical DRH antennas have voltage standing wave ratio (VSWR) less than 2.1 and 2.2 for the frequency ranges of 18–26.5 GHz (K band) and 26.5–40 GHz (Ka band), respectively. Meanwhile, the proposed antennas exhibit low cross-polarization, low sidelobe level, and simultaneously achieve slant polarization as well as symmetrical radiation patterns in the entire operating bandwidth. An exponential impedance tapering is used at the flare section of the horns. Moreover, a new cavity back with a conical structure is used to improve the VSWR. Numerous simulations via Ansoft HFSS and CST Microwave Studio CAD tools have been made to optimize the VSWR performance of the designed antennas. Simulation results show that the VSWR of the proposed antennas is sensitive to the probe spacing from the ridge edge and the cavity back structure. The designed conical DRH antennas are most suitable as a feed for the reflectors of radar systems and satellite applications. Results for VSWR, far-field E-plane and H-plane radiation patterns, and gain of the designed antennas are presented and discussed. Int J RF and Microwave CAE 21:602–610, 2011.

Keywords: DRH; conical antenna; double-ridged; K and Ka frequency bands

I. INTRODUCTION

Horn antennas have received considerable attention for transmission and reception of electromagnetic waves in applications such as reflector feeds, satellite tracking systems, electromagnetic compatibility testing, electronic warfare, radar systems, standard measurements, and detection systems [1–9]. These antennas have several useful properties such as wide bandwidth, versatility, easy excitation, relatively simple construction, relatively high gain, and stable far-field radiation characteristics [10, 11]. The conventional horn antennas have a limited bandwidth. To extend the maximum practical bandwidth of these antennas, ridges are introduced in the flare section of the antenna.

The idea of using ridges in waveguides was adopted in horns by Walton and Sundberg [12], and completed by Kerr in early 1970 when he suggested the use of a feed horn launcher whose dimensions where found experimentally [13]. This is commonly done in waveguides to increase the cutoff frequency of the second propagating mode (TM01) and, thus, expand the single-mode range before higher order modes occur [14–16]. Spreading of higher order modes arises from power division between the modes. Because of various field distributions, they influence the desired radiation patterns and especially the main lobe deteriorates for higher frequencies. In [17, 18], an E-sectoral double-ridged horn antenna (DRH) for broadband application is presented. A detailed investigation on 1–18-GHz broadband pyramidal DRH antenna was reported in [19]. In [20], a broadband electromagnetic compatibility pyramidal DRH antenna for 1–14 GHz was reported. An improved design of the DRH antenna was presented in [21]. Another design of the DRH antenna in the 1–18-GHz frequency range with redesigned feeding section was presented in [22] where several modifications

Correspondence to: H. Abiri; e-mail: abiri@shirazu.ac.ir
DOI 10.1002/mmce.20548
Published online 21 July 2011 in Wiley Online Library (wileyonlinelibrary.com).

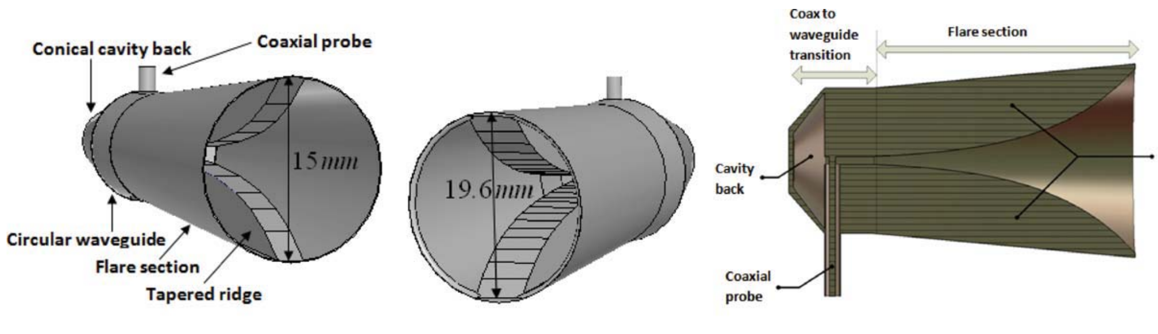

(a) (b) (c)

Figure 1 Configuration of the proposed conical DRH antennas. (a) K-band antenna. (b) Ka-band antenna. (c) cut view of Ka-band antenna. [Color figure can be viewed in the online issue, which is available at wileyonlinelibrary.com.]

were made in the structure of a conventional DRH antenna to overcome the deterioration of its radiation pattern at higher frequencies.

The deterioration of radiation patterns at the high end of the frequency band, cross polarization, back lobe level, and sidelobe level (SLL) are the significant disadvantages of the conventional DRH antennas. Based on the articles available in the open literature, the radiation characteristics of the DRH antennas need to be improved. The proposed conical DRH antennas here do not show the aforementioned disadvantages. Pyramidal DRH antennas have been investigated in many references. There are rare articles in the literature which are devoted to design and analysis of conical DRH antennas in K and Ka bands.

In this article, based on the double-ridged circular waveguide, two conical DRH antennas including 50 Ω coaxial feed, for K and Ka frequency bands are proposed. Accordingly, an exponential impedance tapering is used at the flare section of the horns, and using a coax to waveguide transition with a suitable cavity back structure, the voltage standing wave ratio (VSWR) performance of less than 2.2 for both antennas is obtained. The proposed antennas exhibit low cross polarization, low SLL, and simultaneously achieve slant polarization as well as symmetrical radiation patterns in the entire operating bandwidth. Compared to the conical DRH antenna presented in a previous work [1], the new designed antennas have several attractive advantages, such as higher operating frequency, higher radiation efficiency, better radiation patterns, lower VSWR, lower SLL, and lower back lobe level. Moreover, in this work a new cavity back with a conical structure is used to improve the VSWR. The inner conductor and shield of the coaxial probe should enter very close to the edge of the ridges. Meanwhile, the initial distance between ridges in the circular waveguide and probe spacing from the ridged edge affect the antenna characteristics. Therefore, the fabrication mechanism is important to the antenna characteristics. The designed antennas were fabricated with 0.01 mm accuracy and satisfactory agreement was obtained using computer simulations and experimental results. In the previous work [1], numerical simulations have not been checked experimentally. Numerous simulations have been done to optimize the VSWR performance of the designed antennas. Ansoft HFSS and CST Microwave Studio packages that utilize the finite element and the finite integration techniques respectively are used for simulations. The simulated and measured results for VSWR, far field E-plane and H-plane radiation patterns, and gain of the designed antennas over the frequency band are presented.

II. CONICAL DOUBLE-RIDGED HORN ANTENNA STRUCTURE

The structures of the proposed conical DRH antennas are illustrated in Figure 1. The overall length of the designed antennas for K and Ka frequency bands are 47 and 33.5 mm, respectively. The aperture radius of the one covering K band is 15 mm and the other that covers Ka band is 19.5 mm.

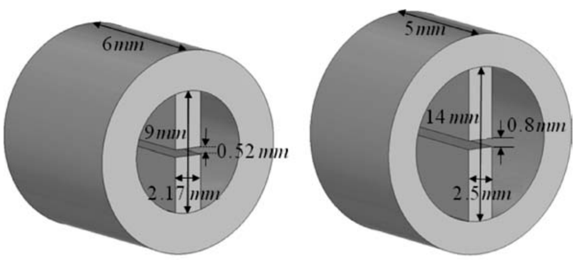

(a) (b)

Figure 2 Double-ridged circular waveguides without coaxial probe. (a) for K band (b) for Ka band.

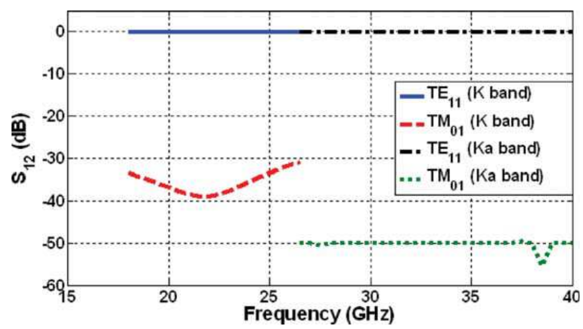

Figure 3 S_{12} parameter of the propagation and nonpropagation modes (TE11 and TM01 modes) versus frequency. [Color figure can be viewed in the online issue, which is available at wileyonlinelibrary.com.]

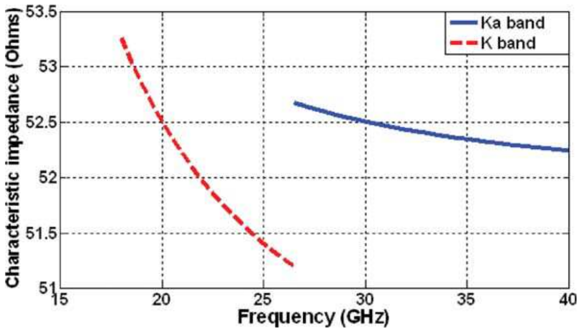

Figure 4 The characteristic impedance of the fundamental propagation mode (TE11 mode) versus frequency. [Color figure can be viewed in the online issue, which is available at wileyonlinelibrary.com.]

In the first step, using Ansoft HFSS the two-port double-ridged circular waveguides without coaxial probe are simulated for the single mode (i.e., TE11 mode) in the K and Ka frequency bands. Figure 2 shows the details of the double-ridged circular waveguides. The S12 parameters of the TE11 and TM01 modes in the double-ridged circular waveguides versus frequency are presented in Figure 3. It can be seen that the lowest mode (i.e., TE11) is the fundamental propagation mode in the waveguides, with the corresponding S12 parameter as 0 dB. Moreover, we observe that the higher order mode (i.e., TM01) with the S12 parameter much lower than 0 dB is not propagating. The characteristic impedance of the fundamental propagation mode, TE11, versus frequency obtained by the Ansoft HFSS is presented in Figure 4. As inferred from this Figure, the characteristic impedance is about 50 Ω, indicating that there is a good impedance matching between the coaxial lines and the double-ridged circular waveguides for single-mode operation in both frequency bands.

Numerous simulations via Ansoft HFSS and CST Microwave Studio have been done to optimize the transitional performance. The principal goal is obtaining low levels of VSWR throughout the transformation of the TEM-mode in the coaxial section to the TE-mode in the waveguide. To have a low VSWR, the cavity back dimensions, the initial distance between the ridges in the circular waveguide as well as the distance between the probe and the edge of the ridge should be optimized. Moreover, the simulation results show that this latter distance affects the antenna gain and the main lobe of the radiation patterns at high frequencies. As is shown in Figure 5, for low return loss, the shield of the coaxial probe is connected to the lower ridge and the inner conductor is connected to the

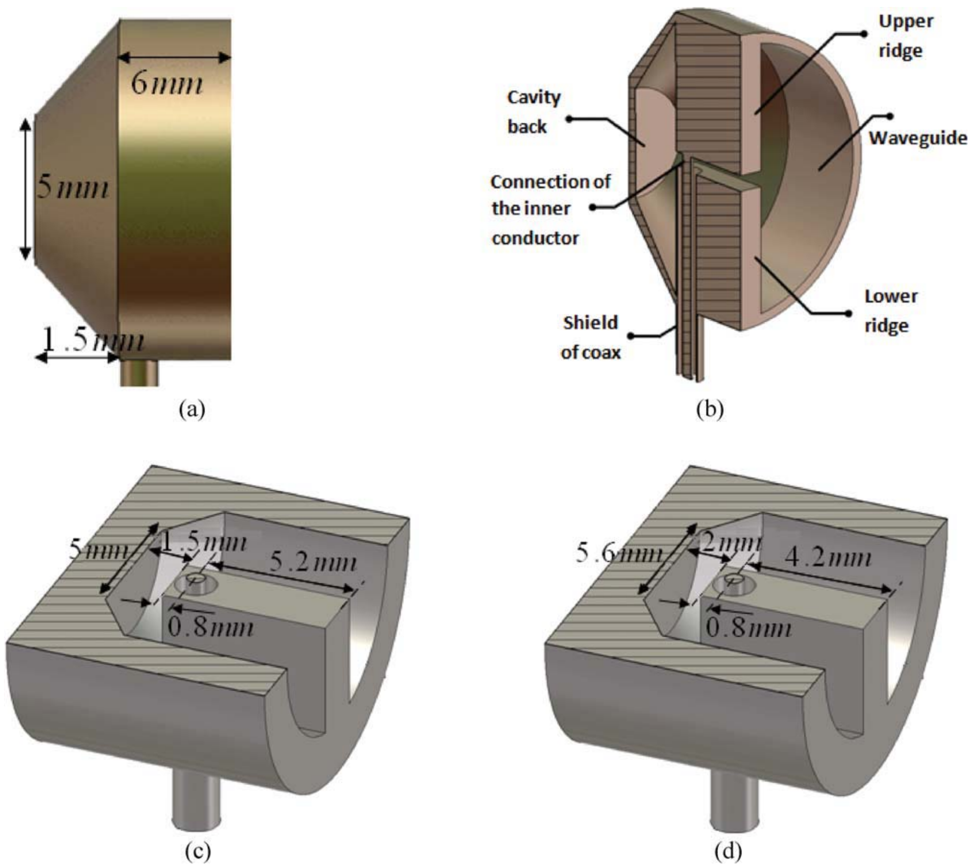

Figure 5 Configuration of the designed coax to double-ridged circular waveguide transition. (a) side view for K band. (b) Vertical cut view for K band. (c) Horizontal cut view for K band. (d) Horizontal cut view for Ka band. [Color figure can be viewed in the online issue, which is available at wileyonlinelibrary.com.]

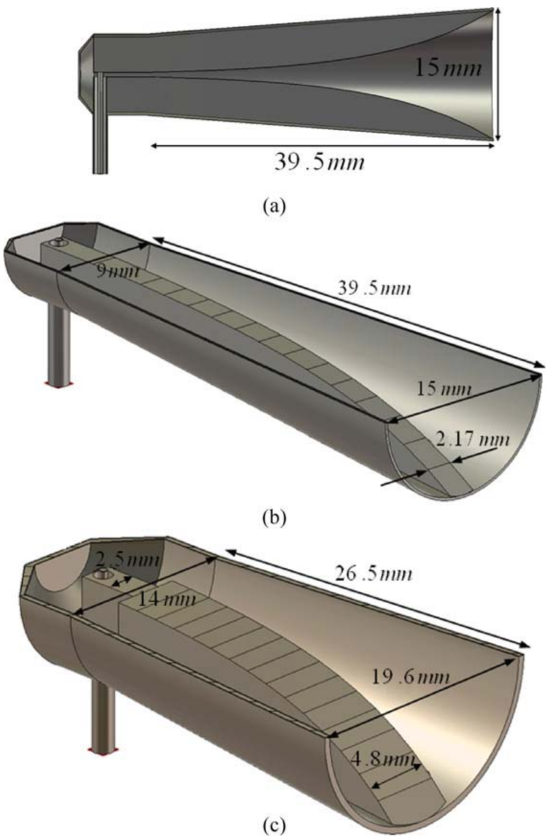

Figure 6 The conical DRH antennas made from 15 smaller waveguides each of different height. (a) Vertical cut view for K band. (b) Horizontal cut view for K band. (c) Horizontal cut view for Ka band. [Color figure can be viewed in the online issue, which is available at wileyonlinelibrary.com.]

upper ridge by passing through a tunnel in the lower ridge. The inner conductor and shield of the coaxial probe should be very close to the edge of the ridges.

A cavity back is commonly used to improve the VSWR of the coax to double-ridged waveguide transition. Simulations show that the VSWR of the proposed antennas is critically sensitive to the structure and dimensions of the cavity back. To improve the VSWR (lower than 2.2), a cavity back with a conical structure is used. The cavity dimensions that are obtained using the optimization tools are shown in Figure 5.

The axial length of the horn opening (flare section) should satisfy the inequality $L > \lambda$, where λ is the wavelength of the center frequency [12]. For the desired gain, $\sim$10–12 dB, over the operating frequency range, the aperture size is determined from the simulation of the horn antenna without the ridges. The length of the horn opening (flare section) for K and Ka frequency bands are 39.5 and 26.5 mm, respectively. As mentioned in [1], the above dimensions are obtained through extensive simulations and optimization to provide the desired bandwidth along with good radiation characteristics. The design of the tapered section is the most significant part in the DRH antenna design. The detailed design of the exponential tapered ridges is explained in [1]. The final shapes of the ridges are exponential like taper and are shown in Figure 6.

III. RESULTS AND DISCUSSION

In this section, we present the simulation and experimental results for the proposed conical DRH antennas. To check the accuracy of simulations, we have compared the outcomes of both simulator packages HFSS and CST. Closed results confirm the accuracy of simulations. To justify the results, the designed antennas were fabricated, tested, and compared with the simulations. The pictures of the fabricated antennas are shown in Figure 7. The horn antennas and the double ridges are fabricated using, aluminum and copper, respectively. Copper is used for the ridges due to increased mechanical strength during machining.

The simulated and measured VSWR of the designed antennas are presented in Figure 8. It is seen that maximum value of the VSWR is less than 2.1 and 2.2 for the frequency ranges 18–26.5 GHz (K band) and 26.5–40 GHz (Ka band), respectively. The discrepancy between theory and experiment is partly due to the fabrication imperfections. The connection of probe causes a capacitive effect which in turn changes the input impedance of the DRH

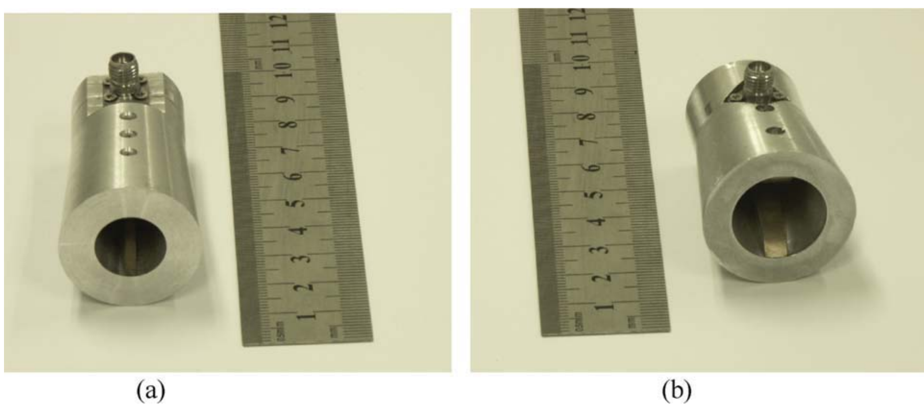

Figure 7 The photographs of the fabricated antennas. (a) K-band antenna. (b) Ka-band antenna. [Color figure can be viewed in the online issue, which is available at wileyonlinelibrary.com.]

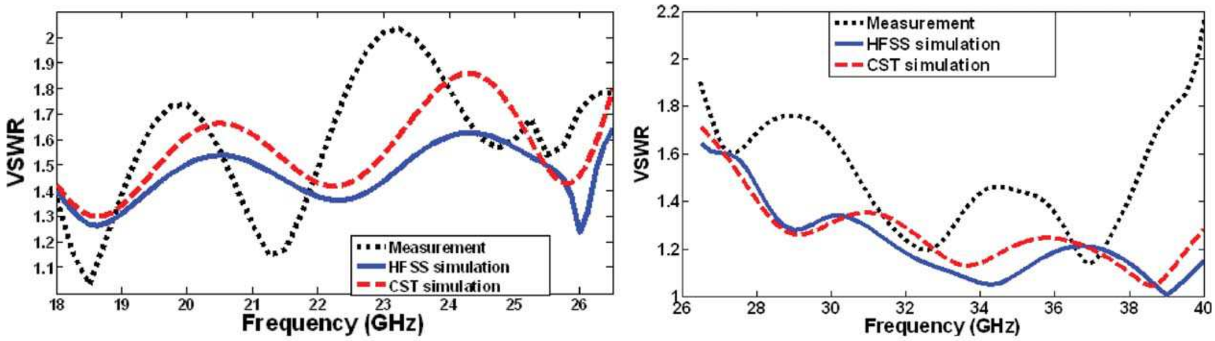

(a) (b)

Figure 8 Simulated and measured VSWR of the proposed antennas. (a) K-band antenna. (b) Ka-band antenna. [Color figure can be viewed in the online issue, which is available at wileyonlinelibrary.com.]

antenna. This effect also contributes to the measurement error. The simulated and measured far-field E-plane ($\varphi = 90^\circ$) and H-plane ($\varphi = 0^\circ$) radiation patterns of the proposed antennas at several typical frequencies are presented in Figures 9 and 10. It can be observed that they have satisfactory radiation patterns with low SLL over the entire frequency band. The cross-polarization level is very important, especially when horn antennas are used as feeds for reflector antennas. The designed antennas provide linear polarization with a cross-polarization level about 40 dB lower than the copolarization level at boresight in all of the measured radiation patterns.

As was mentioned in the introduction, the commercially available ridged horn antennas investigated by the authors displayed significant pattern deterioration at higher frequencies. At higher frequencies, the single main lobe split into some large side lobes that grow around the 0°center axis so that the main lobe appears to be strongly indented. This deterioration, which results in a sudden gain reduction in the E- and H-plane measurements, can be visualized in a three-dimensional (3D) simulated radiation pattern plot [19]. Figure 11 shows the 3D simulated far-field radiation patterns of the proposed antennas. As shown in this figure, the proposed antennas have desirable

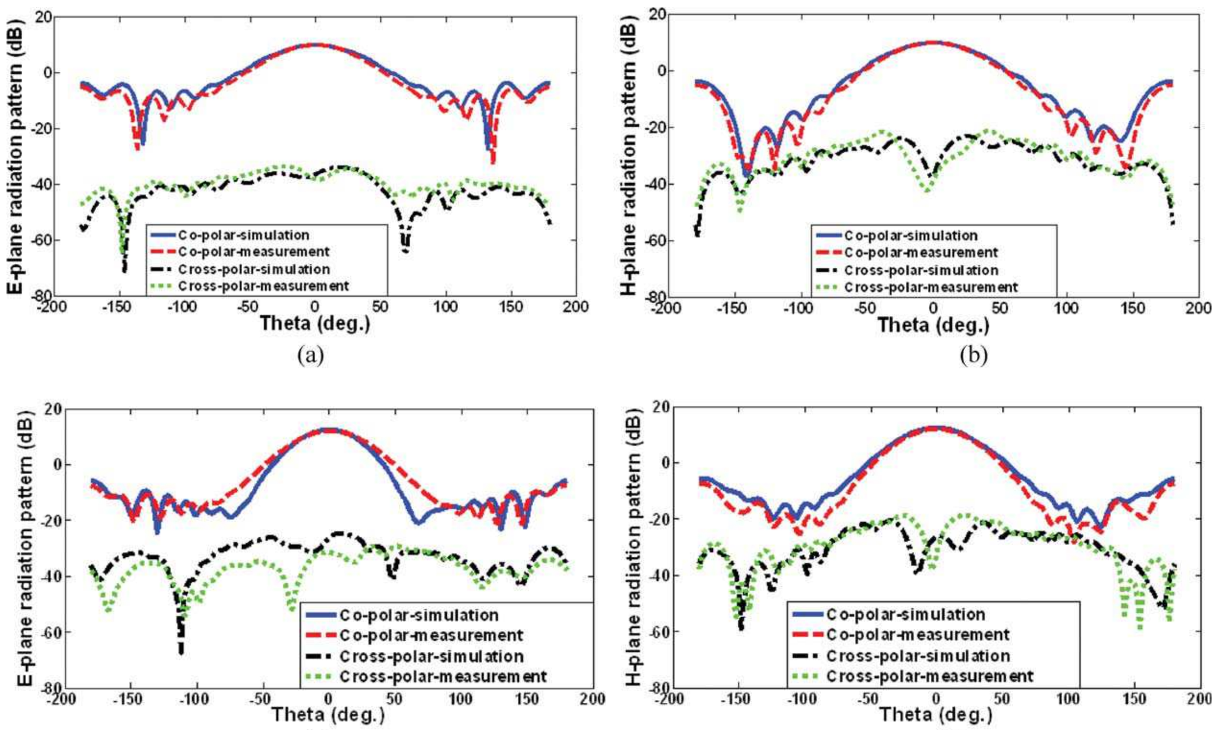

(c) (d)

Figure 9 The simulated and measured radiation patterns of the K-band antenna. (a) E-plane at 18 GHz, (b) H-plane at 18 GHz, (c) E-plane at 26.5 GHz, (d) H-plane at 26.5 GHz. [Color figure can be viewed in the online issue, which is available at wileyonlinelibrary.com.]

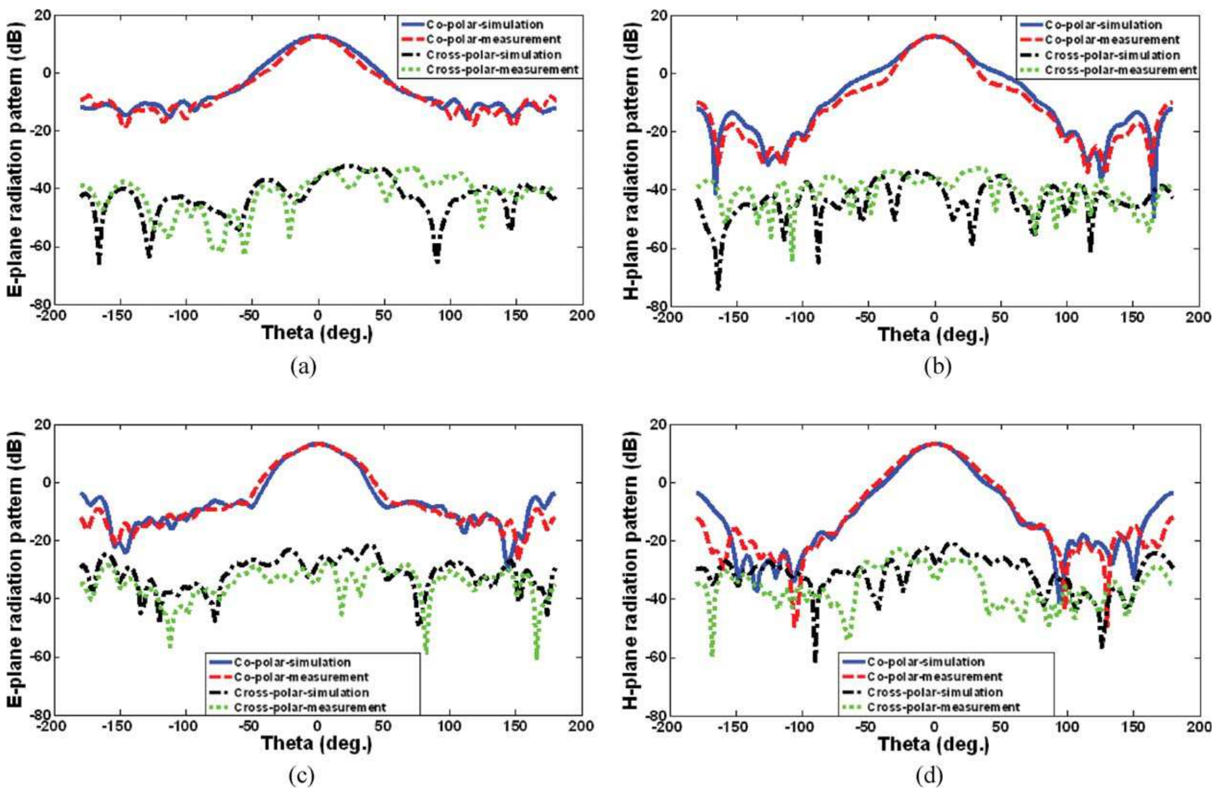

Figure 10 The simulated and measured radiation patterns of the Ka-band antenna. (a) E-plane at 26.5 GHz, (b) H-plane at 26.5 GHz, (c) E-plane at 40 GHz, (d) H-plane at 40 GHz. [Color figure can be viewed in the online issue, which is available at wileyonlinelibrary.com.]

characteristics, i.e., they have one dominant main lobe without squint in the entire frequency band.

In practice, the radiation patterns are presented only in the E- and H-planes and, consequently, just show a gain drop in the broadside direction. The large side lobes, however, will not be detected in a standard E- and H-plane testing procedure and, therefore, do not appear on pattern measurement data sheets [19]. To investigate the existence of the sidelobes, the horn antennas were brought into a 45° azimuthally diagonal position. In this plane, the principal goal is obtaining slant polarization performance. The simulated and measured E_θ and E_ϕ patterns in the diagonal plane ($\varphi = 45°$) at several typical frequencies are shown in Figure 12. This Figure gives useful information about cross-polarization level. In this plane, according to Ludwig's third definition [23], the cross-polarization is equal to $(E_\theta + E_\varphi)/1.414$. It is found that the cross-polarization level in this plane is larger than the standard E- and H-planes as expected. The close values of vertical and horizontal

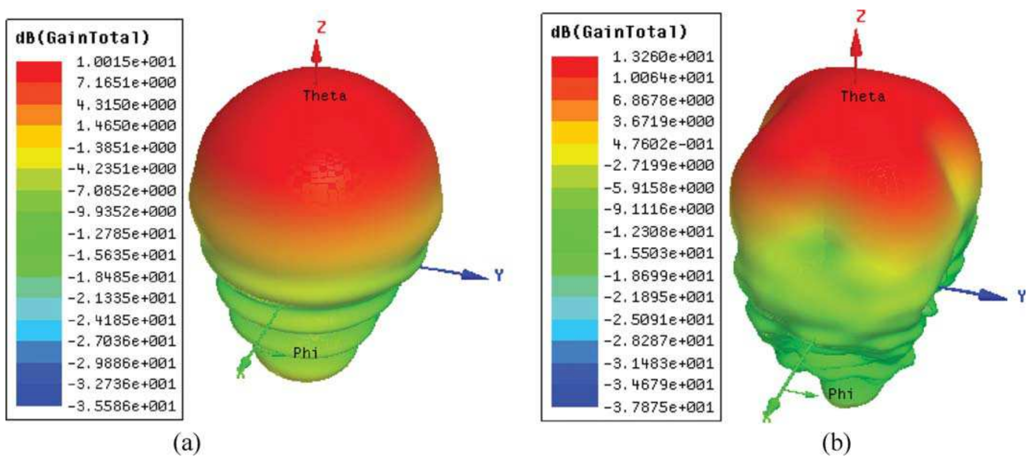

Figure 11 3D far-field radiation patterns of the antennas obtained by Ansoft HFSS. (a) K-band antenna at 18 GHz. (b) Ka-band antenna at 40 GHz. [Color figure can be viewed in the online issue, which is available at wileyonlinelibrary.com.]

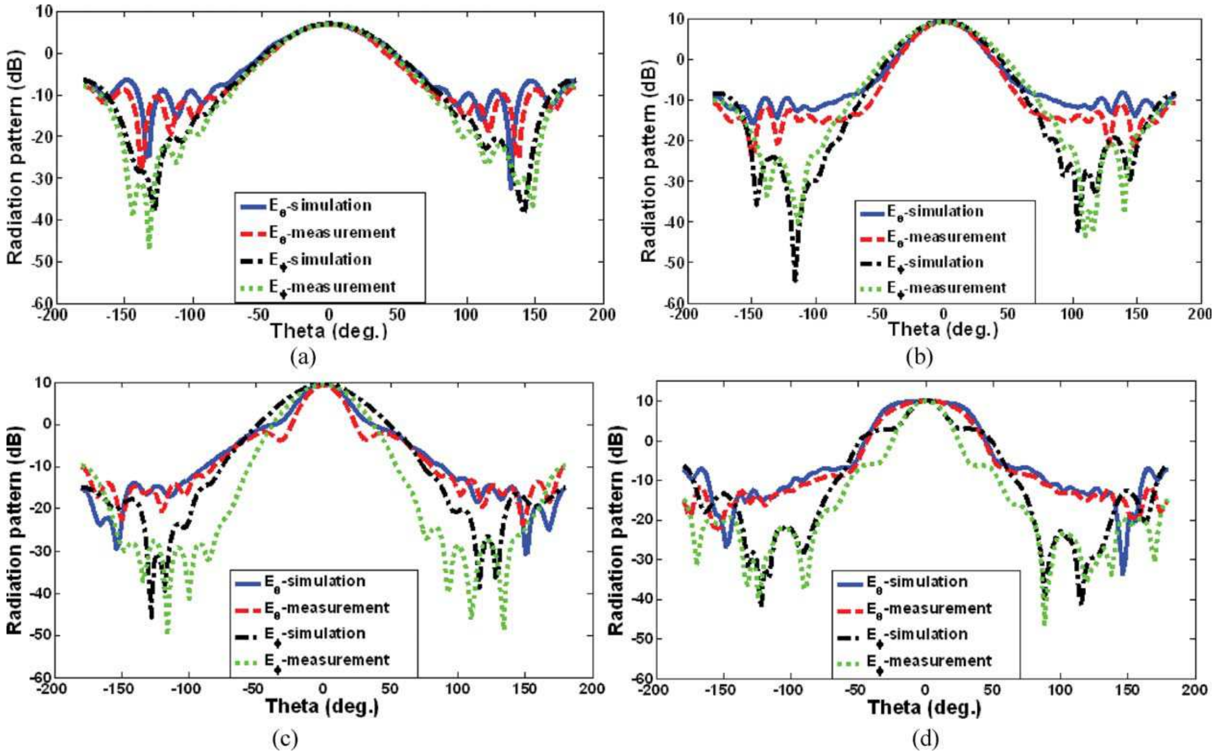

Figure 12 The simulated and measured radiation patterns of the antennas in the diagonal plane. (a) Results for K-band antenna at 18 GHz. (b) Results for K-band antenna at 26.5 GHz. (c) Results for Ka-band antenna at 26.5 GHz. (d) Results for Ka-band antenna at 40 GHz. [Color figure can be viewed in the online issue, which is available at wileyonlinelibrary.com.]

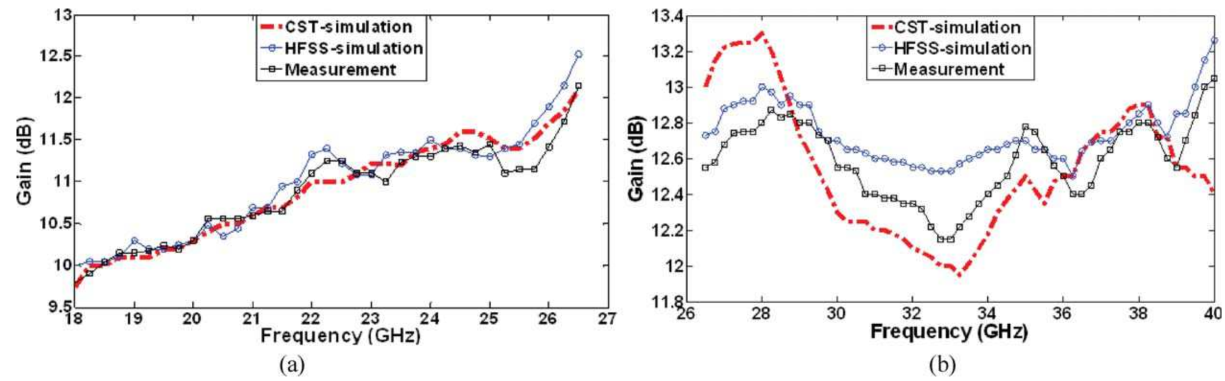

Figure 13 The simulated and measured gains of the antennas versus frequency, (a) Results for K-band antenna. (b) Results for Ka-band antenna. [Color figure can be viewed in the online issue, which is available at wileyonlinelibrary.com.]

gains represent the good performance of the proposed antenna for slant polarization.

The simulated and measured gains of the proposed antennas versus frequency are presented in Figure 13. The antenna peak gain is ~12.2 and 13 dB for K and Ka bands, respectively. The gain variation within the bandwidth is less than about 2.5 dB. The results show that the simulated gain is in good agreement with the measured gain across the entire frequency band. According to these results, the proposed conical DRH antennas can be useful as a feed for the reflectors in broadband direction finder systems, satellite, and communication systems applications.

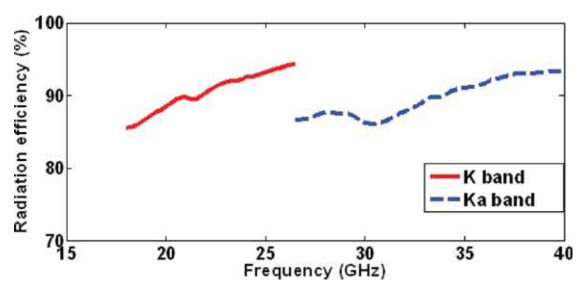

Figure 14 Radiation efficiency calculated from the measured parameters. [Color figure can be viewed in the online issue, which is available at wileyonlinelibrary.com.]

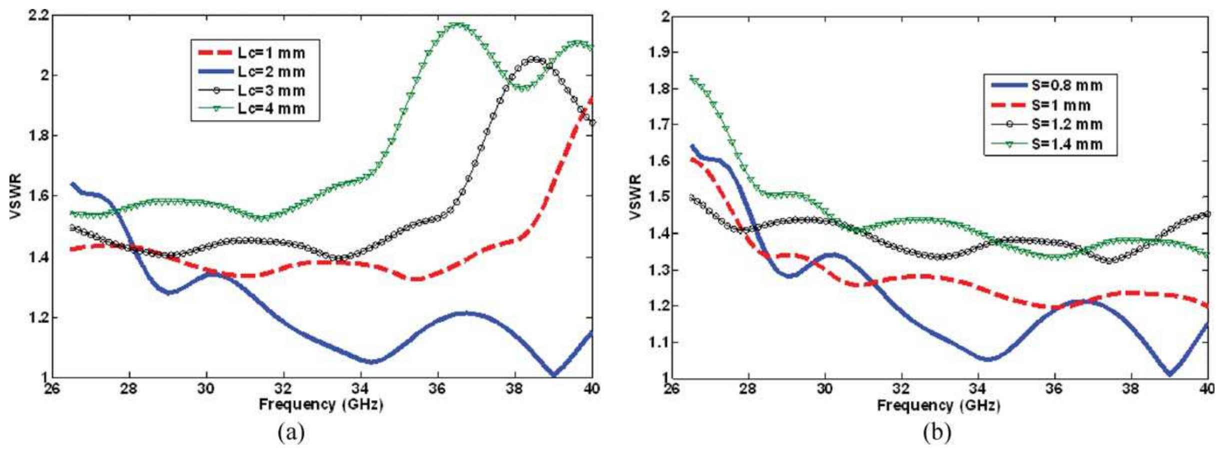

Figure 15 Simulated VSWR (by Ansoft HFSS) of Ka-band antenna (a) for various cavity back length (L_c). (b) For various probe spacing from the ridge edge (S). [Color figure can be viewed in the online issue, which is available at wileyonlinelibrary.com.]

The antenna radiation efficiency can be written as:

$$e = \frac{G}{(1-|\Gamma|^2)D} \quad (1)$$

where G, D, and Γ are gain, directivity, and the reflection coefficient of the antenna, respectively [24]. The simulated radiation efficiency at the center frequency is 96 % and 94 % for K and Ka bands, respectively. For calculation of D based on measured data the following approximate equation is used.

$$D \cong \frac{72815}{\theta_E^2 + \theta_H^2} \quad (2)$$

where θ_E and θ_H are the half-power beamwidths (in degrees) in E- and H-planes, respectively [24]. Figure 14 depicts the calculated radiation efficiency of the antennas. The maximum value of radiation efficiency is ~94.3 and 93.4% for K and Ka bands, respectively. It can be seen that the efficiency variation is around 8.7 and 6.7% over the frequency band.

As mentioned before, the performances of the proposed antennas are sensitive to the probe spacing from the ridge edge and the cavity back structure. The simulated VSWR of Ka-band antenna for various cavity back length (L_c), 1, 2, 3, and 4 mm are presented in Figure 15a. This factor affects the performance of the proposed antenna most effectively. As shown in this figure, the VSWR deteriorates within the whole band as L_c changes. The best value for L_c in the designed antenna is 2 mm. Through extensive simulations, it is found that the VSWR critically depends on the probe spacing from the ridge edge (S). Figure 15b shows the simulated VSWR of the Ka-band antenna for various S values. As the results show, the VSWR varies within the whole band as S value changes. It can be seen that the optimum value of S is 0.8 mm. Based on these results, if this dimensional tolerance in fabrication procedure is not lower than 0.2 mm, the antenna performances deteriorate within the whole band. Although not shown, similar results were obtained for the K-band antenna.

IV. CONCLUSION

Two conical DRH antennas for K- and Ka-frequency bands have been proposed. An exponential impedance tapering is used at the flare section of the horns, and using a coax to waveguide transition with a suitable cavity back structure, the VSWR performance of less than 2.2 for both antennas is obtained. Moreover, the proposed antennas exhibit low cross-polarization, low SLL, and simultaneously slant polarization as well as symmetrical radiation patterns in the entire operating bandwidth. Compared to the conical DRH antenna presented in a previous work, the new designed conical DRH antennas have higher operating frequency band, lower VSWR, higher radiation efficiency, better radiation patterns, lower SLL, and lower back lobe level. In this work, numerical simulations have been checked experimentally and satisfactory agreement is obtained. Ansoft HFSS and CST Microwave Studio packages are used for simulations. Simulation results show that the performances are sensitive to the probe spacing from the ridge edge and the cavity back structure. Based on these characteristics, the proposed conical DRH antennas can be useful as a feed for the reflectors of radar systems, direction finder systems, satellite, and microwave applications.

REFERENCES

1. A.R. Mallahzadeh and A.A. Dastranj, Double-ridged conical horn antenna for wideband applications, Int J RF Microwave CAE 19 (2009), 338–345.
2. A.R. Mallahzadeh, A.A. Dastranj, and S. Akhlaghi, Quad-ridged conical horn antenna for wideband applications, Int J RF Microwave CAE 19 (2009), 519–528.
3. A.R. Mallahzadeh, A.A. Dastranj, and F. Karshenas, Pattern squint elimination for quad-ridged conical and pyramidal horn antennas using bended probes, Int J RF Microwave CAE 20 (2010), 94–102.
4. A.R. Mallahzadeh, A.A. Dastranj, and H.R. Hassani, A novel dual-polarized double-ridged horn antenna for wideband applications, Prog Electromagn Res B 1 (2008), 67–80.
5. A.R. Mallahzadeh and A.A. Dastranj, Double-ridged conical horn antenna for 2–18 GHz, Electromagnetics 28 (2008), 450–461.

6. H. Lai, R. Franks, D. Kong, D. Kuck, and T. Gackstetter, A broad band high efficent quad ridged horn, Antennas Propag Soc Int Symp 5 (1987), 676–679.
7. A. Hizal and U. Kazak, A broadband coaxial ridged horn antenna, Proceedings of 19th European Microwave Conference, Turnbridge Wells, UK, 1989, pp. 247–252.
8. V. Venkatesan and K.T. Selvan, Rigorous gain measurements on wide-band ridge horn, IEEE Trans Electromagn Compat 3 (2006).
9. M. Abbas-Azimi, F. Arazm, and R. Faraji-Dana, Design and optimization of a high frequency EMC wideband horn antenna, IET Microwave Antennas Propag 1 (2007), 580–585.
10. W.L. Barrow and L.J. Chu, Theory of the electromagnetic horn, Proc IRE 27 (1939), 51–64.
11. F.F. Dubrovka, G.A. Yena, P.Y. Stepanenko, and V.M. Tereschenko, Ultra wideband double ridged horn with rectangular aperture, International Conference on Antenna Theory and Techniques, Seuastopol, Ukraine, September 9–12, 2003, pp. 590–593.
12. K.L. Walton and V.C. Sundberg, Broadband ridged horn design, Microwave J 4 (1964), 96–101.
13. J.L. Kerr, Short axial length broad-band horns, IEEE Trans Antennas Propag AP-21 (1973), 710–714.
14. S. Hopfer, The design of ridged waveguides, IRE Trans Microwave Theory Tech MIT- 3 (1955), 20–29.
15. S.B. Cohn, Properties of ridged waveguide, Proc IRE 35 (1947), 783–788.
16. D.A. Jarvis, and T.C. Rao, Design of double-ridged rectangular wave guide of arbitrary aspect ratio and ridge height, IEE Proc Microwave Antenna Propag 147 (2000), 31–34.
17. C. Reig and E. Navarro, FDTD analysis of E-sectoral horn antenna for broadband applications, IEEE Trans Antennas Propag 45 (1997), 1485–1487.
18. R. Bunger, R. Beyer, and F. Arndt, FDTD analysis of E-sectoral horn antennas for broadband applications, IEEE Trans Antennas Propag 47 (1999), 1641–1648.
19. C. Bruns, P. Leuchtmann, and R. Vahldieck, Analysis and simulation of a 1–18 GHz broadband double-ridged horn antenna, IEEE Trans Electromagn Compat 45 (2003), 55–59.
20. M. Botello-Perez, H. Jardon-Aguilar, and I. Ruiz, Design and simulation of a 1 to 14 GHz broadband electromagnetic compatibility DRGH antenna, ICEEE-ICE 2005, 2nd International Conference on Electrical and Electronics Engineering, September 2005, pp. 118–121.
21. V. Rodriguez, New broadband EMC double-ridged guide horn antenna, RF Des 27 (2004), 44–47.
22. M. Abbas-Azimi, F. Arazm, J. Rashed-Mohassel, and R. Faraji-Dana, Design and optimization of a new 1–18 GHz double ridged guide horn antenna, J Electromagn Wave Appl 21 (2007), 501–506.
23. A.C. Ludwig, The definition of cross polarization, IEEE Trans Antennas Propag 21 (1973), 116–119.
24. C.A. Balanis, Antenna theory: Analysis and design, 2rd ed, Wiley, New York, 1997.

BIOGRAPHIES

Aliakbar Dastranj was born in Yasouj, Iran, in 1983. He received the B.Sc. degree in electronic engineering from Shiraz University, Shiraz, Iran, in 2006 and the M.Sc. degree in electrical and communication engineering from Shahed University, Tehran, Iran, in 2008. He is currently working toward the Ph.D. degree at Shiraz University, Shiraz, Iran. From 2006 until April 2008, he was a Teaching Assistant with the Department of Electrical Engineering, Shahed University. Since April 2008, he has been a Research Fellow in the School of Electrical and Computer Engineering, Shiraz University. His research interests include wideband horn antennas, analysis and design of microstrip antennas, design and modeling of microwave structures, and electromagnetic theory. He has published several papers in different international journals and conferences.

Habibollah Abiri received the B.S degree in electrical engineering from Shiraz University, Shiraz, Iran, and the D.E.A. and Doctor Ingenieur degrees from National Polytechnique Institute of Grenoble (INPG), Grenoble, France, in 1978, 1981, and 1984, respectively. In 1985, he was an Assistant Professor with the University of Savoie, Chambery, France. Since 1985, he has been with the Electrical Engineering Department, Shiraz University, where he is now a Professor In 1995, he was on sabbatical leave at the Electrical Engineering Department, Colorado State University, Fort Collins, U.S.A. His research interests include numerical methods in electromagnetic theory, microwave circuits, and integrated optics. Dr. Abiri is a member of the Iranian Association of Electrical and Electronics Engineers.

Alireza Mallahzadeh was born in Bushehr, a beautiful city in the south of Iran, in 1977. He received the B.S. degree in electrical engineering from Isfahan University of Technology, Isfahan, Iran, in 1999, and the M.Sc. degree in electrical engineering from Iran University of Science and Technology, Tehran, in 2001, and the Ph.D. degree in electrical engineering from Iran University of Science and Technology, Tehran, in 2006. He is a member of academic staff, Faculty of Engineering, Shahed University, Tehran. He has participated in many projects relative to antenna design, which resulted in fabricating different types of antennas for various companies. Also, he is interested in numerical modeling and microwaves.